Spin ordering and electronic texture in the bilayer iridate Sr3Ir2O7

Authors: Chetan Dhital, Sovit Khadka, Z. Yamani, Clarina de la Cruz, Thomas C. Hogan, Steven M. Disseler, Mani Pokharel, Kevin C. Lukas, Wei Tian, Cyril P. Opeil, Ziqiang Wang, Stephen Wilson

Published in *Physical Review B*, vol. 86, no. 10, pp. 100401:1-100401:4, September 2012

PHYSICAL REVIEW B **86**, 100401(R) (2012)

Spin ordering and electronic texture in the bilayer iridate $Sr_3Ir_2O_7$

Chetan Dhital,[1] Sovit Khadka,[1] Z. Yamani,[2] Clarina de la Cruz,[3] T. C. Hogan,[1] S. M. Disseler,[1] Mani Pokharel,[1] K. C. Lukas,[1] Wei Tian,[3] C. P. Opeil,[1] Ziqiang Wang,[1] and Stephen D. Wilson[1,*]

[1]*Department of Physics, Boston College, Chestnut Hill, Massachusetts 02467, USA*

[2]*Chalk River Laboratories, Canadian Neutron Beam Centre, National Research Council, Chalk River, Ontario, Canada K0J 1P0*

[3]*Neutron Scattering Science Division, Oak Ridge National Laboratory, Oak Ridge, Tennessee 37831-6393, USA*

(Received 7 June 2012; published 7 September 2012)

Through a neutron scattering, charge transport, and magnetization study, the correlated ground state in the bilayer iridium oxide $Sr_3Ir_2O_7$ is explored. Our combined results resolve scattering consistent with a high temperature magnetic phase that persists above 600 K, reorients at the previously defined $T_{AF} = 280$ K, and coexists with an electronic ground state whose phase behavior suggests the formation of a fluctuating charge or orbital phase that freezes below $T^* \approx 70$ K. Our study provides a window into the emergence of multiple electronic order parameters near the boundary of the metal to insulator phase transition of the $5d$ $J_{\text{eff}} = 1/2$ Mott phase.

DOI: 10.1103/PhysRevB.86.100401 PACS number(s): 75.25.Dk, 75.50.Ee, 72.20.Ht

There has been considerable interest recently in studying the phase behavior of correlated $5d$-electron transition metal oxides due to the potential of realizing electronic phenomena possible only when electron hopping, spin-orbit coupling, and Coulomb interaction energy scales are almost equivalent.[1–3] Of particular focus has been members of the iridium oxide Ruddelsden-Popper (RP) series $Sr_{n+1}Ir_nO_{3n+1}$, where an experimental picture of a spin-orbit induced $J_{\text{eff}} = 1/2$ Mott insulating state has been proposed.[4,5] Upon increasing the dimensionality of the iridate RP series to higher n, optical[6] and transport measurements[7,8] have shown that the effective bandwidth increases and the system transitions from a quasi-two-dimensional insulating state to a metallic phase in the three-dimensional limit.

Specifically, the reported optical gap in the $n = 2$ member $Sr_3Ir_2O_7$ (Sr-327) shifts considerably downward relative to the $n = 1$ Sr_2IrO_4 system into what should be a weakly insulating phase,[6] demonstrating that Sr-327 occupies a unique position in the iridate RP phase diagram near the boundary of the metal to insulator phase transition in the RP series. Given this framework, $Sr_3Ir_2O_7$ exhibits a number of anomalous features in its magnetic properties: Bulk magnetization measurements of Sr-327 reveal a rich behavior possessing three distinct energy scales,[8,9] and recent muon spin rotation (μSR) measurements have revealed the presence of highly disordered local spin behavior,[10] both supporting the notion of multiple coexisting or competing magnetic phases. However, the details of how spin order evolves in this material and interfaces with the energy scales identified in both transport and bulk susceptibility measurements remains largely unexplored.

In this Rapid Communication, we utilize neutron scattering, bulk magnetization, and transport techniques to explore the phase behavior in $Sr_3Ir_2O_7$ (Sr-327). At high temperatures, a phase appears with $T_{\text{onset}} > 600$ K followed by a second magnetic transition at $T_{AF} = 280$ K. Scattering from this high temperature phase is consistent with a magnetic origin, provides an explanation for the absence of Curie-Weiss paramagnetism in this material above 280 K,[11] and also suggests an origin for the recently reported anomalous 93 meV magnon gap.[12] At low temperatures, the spin order is decoupled within resolution from a second upturn in the bulk spin susceptibility at $T_O = 220$ K, suggestive of the formation of an electronic glass that freezes below $T^* \approx 70$ K. Below this freezing energy scale, charge transport demonstrates a localized ground state that can be biased into a regime of field enhanced conductivity (FEC) consistent with collective transport above a threshold electric field. Our combined results demonstrate the coexistence of spin order with an unconventional, electronically textured, phase in an inhomogeneous ground state near the boundary but on the insulating side of the $J_{\text{eff}} = 1/2$ Mott transition.

Single crystals of $Sr_3Ir_2O_7$ (Sr-327) were grown via flux techniques similar to earlier reports.[13,14] The resulting Sr:Ir ratio was confirmed to be 3:2 via energy dispersive spectroscopy (EDS) measurements, and a number of Sr-327 crystals were also ground into a powder and checked via x-ray diffraction in a Bruker D2 Phaser system. No coexisting Sr_2IrO_4 phase was observed and the resulting pattern was refined to the originally reported $I4/mmm$ structure—we note, however, that, due to the small scattering signal from oxygen, we are unable to distinguish between this and the various reported orthorhombic symmetries.[8,11,13] For the remainder of this Rapid Communication, we will index the unit cell using the pseudotetragonal unit cell with $a = b = 5.50$ Å, $c = 20.86$ Å.

Neutron measurements were performed on the HB-1A triple-axis spectrometer at the High Flux Isotope Reactor (HFIR) at Oak Ridge National Laboratory and on the C5 spectrometer at the Canadian Neutron Beam Centre at Chalk River Laboratories. Experiments on C5 were performed with a vertically focusing pyrolitic graphite (PG-002) monochromator and analyzer, an $E_f = 14.5$ meV, two PG filters after the sample, and collimations of 33′-48′-51′-144′ before the monochromator, sample, analyzer, and detector, respectively. On HB-1A, a double bounce PG monochromator was utilized with fixed $E_i = 14.7$ meV, two PG filters before the sample, and collimations of 48′-48′-40′-68′. Magnetization measurements were performed on a Quantum Design MPMS-XL system and resistivity data was collected in a series of four-wire setups: (1) Zero field resistance from 300 to 12 K was collected

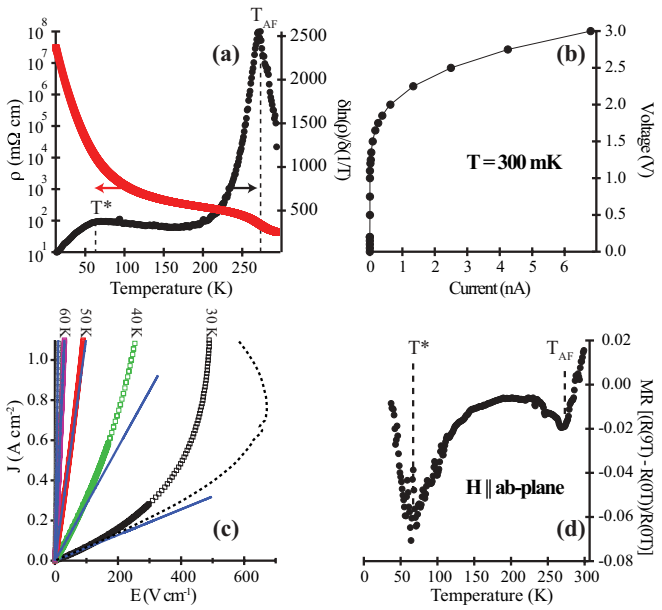

FIG. 1. (Color online) (a) Temperature dependence of the *ab*-plane resistivity for Sr-327. Also plotted is the $\frac{\partial \ln \rho}{\partial (1/T)}$ vs T showing two peaks at T_{AF} and T^*. (b) I-V curve of *ab*-plane transport at 300 mK showing voltage biasing into a FEC regime. (c) Current driven, pulsed, I-V measurements as a function of temperature. Solid lines show linear fits to the Ohmic regime at each temperature. The dashed line is a Joule heating model at 30 K as described in the text. (d) Magnetoresistance (MR) ratio as described in the text plotted as a function of temperature showing two well defined minima at the T^* and T_{AF} transitions.

with a Keithley 2182A voltmeter, (2) data from 12 to 0.3 K was collected in a ^{3}He absorption refrigerator with an Keithley Model 617 electrometer, and (3) magnetoresistance data was collected in a 9 T Quantum Design PPMS.

Looking first at the results of our *ab*-plane transport measurements under low (1 μA) current, Fig. 1(a) shows the zero field resistivity as a function of temperature. The sample's resistivity increases from several mΩ cm at room temperature to beyond 10 MΩ cm below 20 K, and begins to show saturation behavior below 2 K.[14] There is no substantial interval of constant activation energy, as illustrated by the overplot of $\frac{\partial \ln \rho}{\partial (1/T)}$ versus T in this same panel. Instead, $\frac{\partial \ln \rho}{\partial (1/T)}$ shows two peaks suggestive of two phase transitions coupling to charge carriers: the first near the known magnetic phase transition at $T_{AF} = 280$ K (Ref. 8) and the second indicating a lower temperature phase formation at $T^* \approx 70$ K.

In order to investigate further the transport properties of this lower temperature, T^* phase, the charge transport was characterized via a voltage driven I-V sweep at 300 mK shown in Fig. 1(b). A pronounced nonlinearity appears, where with increasing field strength the system switches from a linear, Ohmic regime with near zero conductance into a highly non-Ohmic FEC regime. To determine the temperature evolution of this FEC feature, a separate sample was mounted and probed with 600 μs current pulses to minimize heating effects [Fig. 1(c)]. While it is difficult to completely preclude all heating effects within the rise and sample time of the pulse, these pulsed measurements show that the nonlinear bend in the I-V curve persists and eventually vanishes below resolution at $T \approx 60$ K.

A separate (rough) check for discriminating the nonlinear conduction from simple Joule heating can be performed by looking at the 30 K data in Fig. 1(c). The Ohmic regime $R(30\text{ K}) = 42$ kΩ and the maximum pulsed current (2 mA) during the 600 μs pulse delivers a maximum $\Delta Q = 10.1 \times 10^{-5}$ J. While low temperature heat capacity data are needed for Sr-327, as a lower estimate, the heat capacity of Sr_2IrO_4 at 30 K can be used ($\approx$14 J/K),[15] giving a maximum $\Delta T = 5.5$ K (for a 1.32×10^{-6} mol sample). In carrying out a similar analysis for each current value pulsed at 30 K and assuming *perfect* thermal isolation, the measured Ohmic $R(T)$ can be used to determine the lowest fields possible due to pure Joule heating as a function of the pulsed current density. This limiting case is plotted as a dashed line in Fig. 1(c), demonstrating that the nonlinear feature at 30 K is intrinsic.[16]

In looking at the magnetoresistance of the same sample plotted in the Fig. 1(d), the MR $= [R(9\text{ T}) - R(0\text{ T})]/R(0\text{ T})$ ratio is negative and shows two minima at $T^* \approx 70$ K and $T_{AF} = 280$ K. The lower minimum appears approximately at the temperature where the onset of FEC emerges and coincides with the low-T peak in $\frac{\partial \ln \rho}{\partial 1/T}$. The origin of the negative magnetoresistance is likely the removal of spin disorder scattering due to biased magnetic domain populations which will be discussed later, and the inflection below T^* supports the idea of a field coupled order parameter freezing below 70 K. The suppression of enhanced fluctuations originating from an additional electronic instability, however, may also account for the overall negative MR.

Magnetization data shown in Fig. 2(a) supports the idea of a bulk phase transition below 70 K where a downturn in the dc susceptibility originally reported by Cao *et al.*[8] begins, suggestive of a glassy freezing process. Consistent with earlier reports,[8,9] three energy scales are apparent in the field cooled magnetization data: a canted AF phase transition at $T_{AF} = 280$ K, a sharp upturn at $T_O = 220$ K, and an eventual decrease in susceptibility below $T^* = 70$ K. Both field cooled (FC) and zero field cooled (ZFC) data show similar downturns near T^* and an irreversibility temperature near T_O. At 300 K, however,

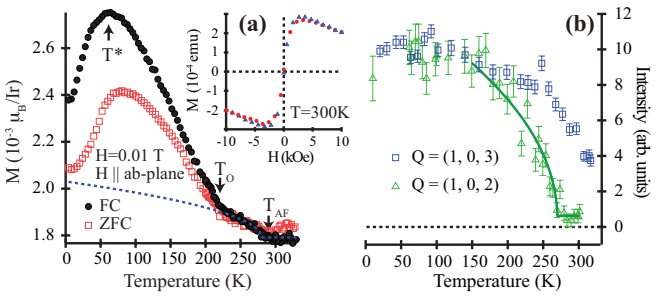

FIG. 2. (Color online) (a) dc-magnetization data for Sr-327 with $H = 0.01$ T aligned parallel to the *ab* plane for both FC (solid symbols) and ZFC temperature sweeps (open symbols). The dashed line shows the mean-field order parameter fit to the net moment from the 280 K transition. The inset shows M vs H sweep at 300 K. (b) Temperature dependence of the peak intensities at (1,0,3) and (1,0,2) magnetic reflections. The solid line is a power law fit to the (1,0,2) order parameter.

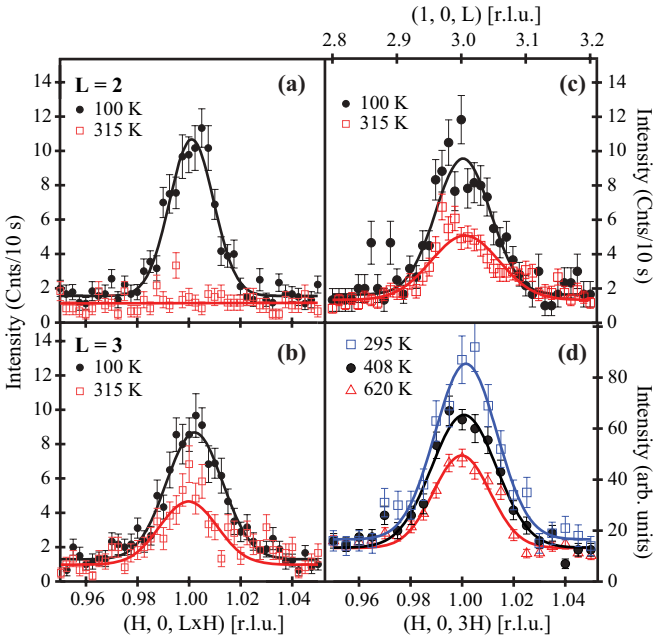

FIG. 3. (Color online) Radial **Q** scans at 100 and 315 K through the (a) **Q** = (1,0,2) and (b) **Q** = (1,0,3) reflections. Solid lines are Gaussian fits to the data. (c) L scans across the (1,0,3) peak position showing three-dimensional (3D) superlattice peaks at 100 and 315 K. (d) **Q** scans showing the temperature dependence of the (1,0,3) peak.

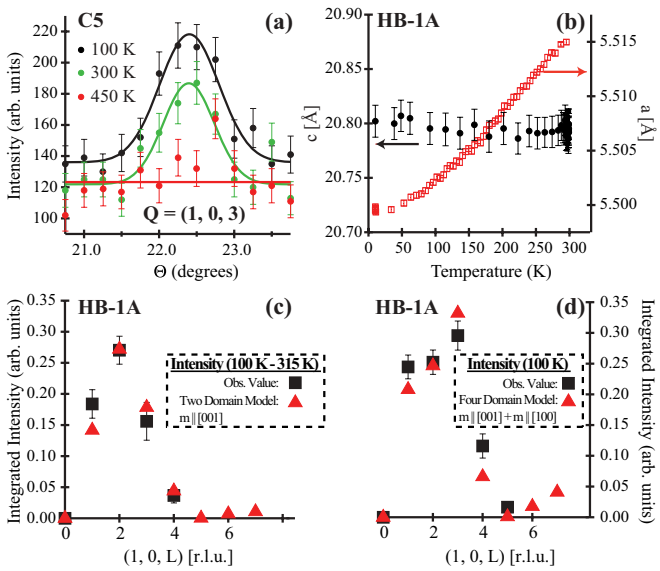

FIG. 4. (Color online) (a) Rocking scans on a separate crystal showing the temperature dependence of the (1,0,3) peak above 300 K. (b) Temperature dependence of the a- and c-axis lattice parameters measured at the (2,0,0) and (0,0,4) reflections. Integrated intensities plotted as (c) 100 K with 315 K data subtracted and (d) the total scattering data at 100 K. Data is compared with two simple collinear spin models described in the text.

field sweeps plotted in the inset of Fig. 2(a) reveal a rapid saturation of the spin response, suggesting the persistence of magnetic correlations above T_{AF}.

In order to further investigate the spin order, neutron diffraction measurements were performed on a 7 mg single crystal Sr-327 sample with the results plotted in Figs. 3 and 4. $[H,0,L]$, $[H,K,0]$, and $[H,H,L]$ zones were explored and magnetic reflections were observed only at the $(1,0,L)$ positions for $L = 1,2,3,4,5$. The correlated order is three dimensional with $\xi_L = \sqrt{2\ln(2)} \times 1/w = 147 \pm 10$ Å, where $w(\text{Å}^{-1})$ is the peak's Gaussian width [Fig. 3(c)]. The appearance of both $L =$ even and $L =$ odd reflections in a simple collinear picture of the spin structure is therefore consistent with recent x-ray results resolving the presence of two magnetic domains.[9] attributable to in-plane structural twinning in an orthorhombic symmetry.

Looking at the order parameters for both the $L = 3$ and $L = 2$ reflections in Fig. 2(b), the magnetic intensities show that the $L = 2$ peak disappears at T_{AF} while substantial intensity remains at 280 K in the $L = 3$ reflection. **Q** scans plotted in Fig. 3(b) demonstrate this more explicitly. The peak remaining above 280 K is long-range ordered with a minimum correlation length of 93 ± 18 Å, comparable to the correlation length observed at 10 K (97 ± 5 Å). Due to the rather coarse collimations used, both these values and those of all magnetic Bragg reflections are resolution limited. At 300 K peaks remain at the $(1,0,L)$ $L = 1,3,4$ positions, all forbidden in the reported structural space groups to date. This same crystal was then loaded into a furnace and measured at higher temperatures, where, upon warming, the remnant peaks continue to decrease in intensity as illustrated in Fig. 3(d); however, they notably remain present beyond 600 K. The continued temperature dependence of these peaks above 300 K and the absence of peaks at higher order L and H strongly imply that this remnant scattering is magnetic and that an additional magnetic phase persists beyond 280 K.

In order to verify this in a second sample, a 2 mg crystal from a separate batch was explored on the C5 spectrometer with the results plotted in Fig. 4(a). Again, a clear temperature dependence above 300 K was observed with the remnant (1,0,3) peak vanishing within the error of the measurement by 450 K. The earlier disappearance of this high temperature AF peak is likely due to the poorer statistics in the measurement of this second sample; however, variable oxygen stoichiometry between samples may also play a role in diminishing the effective transition temperature.

Due to the presence of two magnetic domains[9] and the rapid attenuation due to the Ir magnetic form factor, it is difficult to uniquely determine a model of the spin structure in both the high and low temperature magnetic phases. If we assume that the scattering seen at 315 K is a separate, saturated, order parameter, then the additional intensity due to the 280 K transition is plotted in Fig. 4(c). The rapid disappearance of magnetic peaks for $L > 5$ suggests a sizable component of the moment directed along the c axis, and the best symmetry bound two-domain model matching the data is a G-type arrangement of AF-coupled bilayers with moments directed along the (0,0,1) axis, consistent with a recent x-ray report.[14,17] The ordered moment using this model is $\mu = 0.52 \pm 0.08\mu_B$.

Looking instead at the total scattering observed at 100 K in Fig. 4(d), no simple collinear model captures all of the major reflections well. Nevertheless, if we again use a twinned G-type spin structure, a model comprising four magnetic domains with

two different moment orientations can be constructed. If the two twin domains added to the previous model have moments directed along the (1,0,0) axis, this four domain model roughly fits the data.[14] This added domain would comprise the high temperature phase in a two domain picture, however, future polarized measurements are required to differentiate between this multidomain picture, a potential noncollinear spin structure with an accompanying spin reorientation at 280 K, and to confirm the magnetic nature of the high temperature phase.

Our combined data demonstrate the presence of canted 3D antiferromagnetic domains whose phase evolution is decoupled within resolution from the fluctuation and freezing behavior at T^* and T_O [Fig. 2(b)], precluding any additional major spin reorientations at these temperatures. This suggests that there remain additional moments weakly coupling[8,9] to fluctuations below T_O and eventually freezing below T^*. Our measurements in their entirety therefore suggest a picture of three distinct order parameters driving the phase behavior of Sr-327: (1) a high temperature phase (of likely magnetic origin) with $T_{onset} > 620$ K, (2) a canted AF magnetic transition at 280 K, followed by (3) the freezing of the T^* phase into an electronically textured ground state.

The T^* transition is nominally suggestive of a charge density wave (CDW) or collective transport mechanism which becomes depinned above a threshold field, leading to an avalanche process in the carrier number. The structural lattice parameters [Fig. 4(b)], however, evolve smoothly as the system is cooled from 315 to 10 K and, to date, no structural distortion associated with a conventional CDW formation has been observed below 300 K,[11,18] although, high temperature structural measurements are a promising avenue for future studies. An alternative scenario of exchange coupled metallic islands condensing below T^* with a substantial Coulomb barrier for tunneling may also address the transport mechanism below T^*.[19,20] Similar non-Ohmic behavior has also been reported in other correlated iridates,[21,22] suggesting an electronic inhomogeneity intrinsic to these 5*d*-correlated materials.

Curiously, X-ray measurements on a Sr-327 sample with a qualitatively similar bulk spin susceptibility have reported the onset of AF order at T_O.[9] This resonant x-ray scattering (RXS) study speculated about the presence of short-range order setting in at T_{AF} and diverging at T_O as the reason for the discrepancy,[9] however, our measurements reveal no appreciable change in the correlation length upon cooling through T_O. Given that more recent RXS measurements show the onset of magnetism at the expected $T_{AF} = 285$ K,[17] variation in sample quality is likely the cause for the variance reported between these two RXS studies.

To summarize, our studies have illustrated a complex electronic ground state in the $Sr_3Ir_2O_7$ system with multiple electronic order parameters. Our observation of scattering consistent with an AF phase extending beyond 600 K is supported by the absence of Curie-Weiss behavior above the previously identified T_{AF} (Ref. 11) and also by the rapid field-induced saturation of the magnetization at 300 K. The system then transitions through a magnetic transition at $T_{AF} =$ 280 K, and exhibits multiple magnetic domains or alternatively noncollinear spin order in its ground state. The spin order appears decoupled from two additional energy scales appearing in transport and bulk susceptibility measurements, suggesting a fluctuating charge/orbital state that freezes into an inhomogeneous electronic ground state where tunneling and sliding effects manifest under increasing electric field strength.

S.D.W. acknowledges helpful discussions with Ying Ran and Stefano Boseggia, and Michael Graf for use of a ^{3}He refrigerator. The work at BC was supported by NSF Award DMR-1056625 and DOE DE-SC0002554. Part of this work was performed at ORNL's HFIR, sponsored by the Scientific User Facilities Division, Office of Basic Energy Sciences, US DOE.

*stephen.wilson@bc.edu

[1] B.-J. Yang and Y. B. Kim, Phys. Rev. B **82**, 085111 (2010).
[2] D. A. Pesin and L. Balents, Nat. Phys. **6**, 376 (2010).
[3] F. Wang and T. Senthil, Phys. Rev. Lett. **106**, 136402 (2011).
[4] B. J. Kim *et al.*, Phys. Rev. Lett. **101**, 076402 (2008).
[5] B. J. Kim *et al.*, Science **323**, 1329 (2009).
[6] S. J. Moon *et al.*, Phys. Rev. Lett. **101**, 226402 (2008).
[7] J. M. Longo, J. A. Kafalas, and R. J. Arnott, J. Solid State Chem. **3**, 174 (1971).
[8] G. Cao, Y. Xin, C. S. Alexander, J. E. Crow, P. Schlottmann, M. K. Crawford, R. L. Harlow, and W. Marshall, Phys. Rev. B **66**, 214412 (2002).
[9] S. Boseggia, R. Springell, H. C. Walker, A. T. Boothroyd, D. Prabhakaran, D. Wermeille, L. Bouchenoire, S. P. Collins, and D. F. McMorrow, Phys. Rev. B **85**, 184432 (2012).
[10] I. Franke, P. J. Baker, S. J. Blundell, T. Lancaster, W. Hayes, F. L. Pratt, and G. Cao, Phys. Rev. B **83**, 094416 (2011).
[11] I. Nagai *et al.*, J. Phys.: Condens. Matter **19**, 136214 (2007).
[12] J. Kim *et al.*, arXiv:1205.5337.
[13] M. A. Subramarian, M. K. Crawford, and R. L. Harlow, Mater. Res. Bull. **29**, 645 (1994).
[14] See Supplemental Material at http://link.aps.org/supplemental/10.1103/PhysRevB.86.100401 for additional details.
[15] N. S. Kini *et al.*, J. Phys.: Condens. Matter **18**, 8205 (2006).
[16] Both higher field pulsed measurements and dc measurements show pronounced regions of negative differential resistance; however, for the purpose of this Rapid Communication, we limit our discussion to only measurements where the effect of Joule heating has been minimized.
[17] J. W. Kim, Y. Choi, J. Kim, J. F. Mitchell, G. Jackeli, M. Daghofer, J. van den Brink, G. Khaliullin, and B. J. Kim, Phys. Rev. Lett. **109**, 037204 (2012).
[18] H. Matsuhata *et al.*, J. Solid State Chem. **177**, 3776 (2004).
[19] D. P. Arovas, F. Guinea, C. P. Herrero, and P. San Jose, Phys. Rev. B **68**, 085306 (2003).
[20] P. San-Jose, C. P. Herrero, F. Guinea, and D. P. Arovas, Eur. Phys. B **54**, 309 (2006).
[21] G. Cao, J. Bolivar, S. McCall, J. E. Crow, and R. P. Guertin, Phys. Rev. B **57**, R11039 (1998).
[22] G. Cao *et al.*, Solid State Commun. **113**, 657 (2000).